GEOPHYSICS, VOL. 35, NO. 3 (JUNE 1970), P. 476–489, 14 FIGS.

# ELECTROMAGNETIC INVESTIGATION OF THE SEA FLOOR†

J. H. COGGON* AND H. F. MORRISON*

Numerical evaluation of integral expressions for the fields about a vertical magnetic dipole in the sea allows analysis of the electromagnetic response over wide ranges of sea induction number and sea floor conductivity.

Our analysis indicates that a marine electromagnetic system for measurement of bottom conductivity variations could readily be designed, with such applications as oceanographic and geologic studies, and mineral exploration.

For a source-receiver system on a homogeneous sea bottom, it is found that: (i) when the ratio $k$ = (sea-bed conductivity)/(seawater conductivity) is greater than about 0.03, both horizontal and vertical magnetic fields are useful for measurement of bottom conductivity at sea induction numbers less than 30 [induction number $= \sqrt{2}$ (horizontal transmitter-receiver separation/skin depth)]. A separation of 30 m and frequencies in the range 300–3500 hz appear suitable for investigation of the upper few meters of unconsolidated bottom sediments.

(ii) When the ratio $k$ is less than 0.03, sea induction numbers from 10 to a few hundred are required for detection of seabed conductivity variations. In this case, the horizontal magnetic field, resulting from energy transmission mainly through the seafloor, is the suitable field to use. Electromagnetic sounding of indurated rocks may thus call for frequencies of 100 to 20,000 hz at a separation of 200 m.

Field strengths vary strongly with relative sea depth $D/R$ ($D$ = sea depth, $R$ = horizontal source-receiver separation) when $D/R$ is small; but sensitivity to bottom conductivity is little affected by $D/R$. Elevation of source and receiver above a seafloor less conductive than seawater reduces field strengths and sensitivity to seabed properties.

## INTRODUCTION

With increasing interest and activity in investigating marine resources it is natural to ask what part electromagnetic geophysical techniques may play. Surprisingly little appears to have been done, either experimentally or theoretically, in studying the feasibility of marine application of electromagnetic techniques. Communication problems between submerged stations (including submarines) have received more attention: a concise summary of the feasibility of radio communication in the sea is given by Moore (1967). Beside transmission through the air, propagation below the sea bottom and deeper within the crust has been considered for communication purposes (Mott and Biggs, 1963; Burrows, 1963). The concepts of electromagnetic propagation derived are useful but relate to the far field (intermediate and asymptotic ranges defined by Baños, 1966), whereas near field behavior is commonly important in geophysical systems designed for studying local geology.

Natural fields have been considered for seabed investigation by Brock-Nannestad (1965). A difficulty may be the small size of the fields. Bannister (1968a) showed that the horizontal magnetic field from a line source at the sea surface, measured at the bottom, is sensitive to seabed conductivity. In other papers (1967, 1968b), he derived solutions for dipole fields and found

† Presented at the 39th Annual International SEG Meeting, Calgary, 1969. Manuscript received by the Editor November 24, 1969; revised manuscript received March 6, 1970.

* Department of Materials Science and Engineering, University of California, Berkeley, California 94720.

Copyright ©1970 by the Society of Exploration Geophysicists.

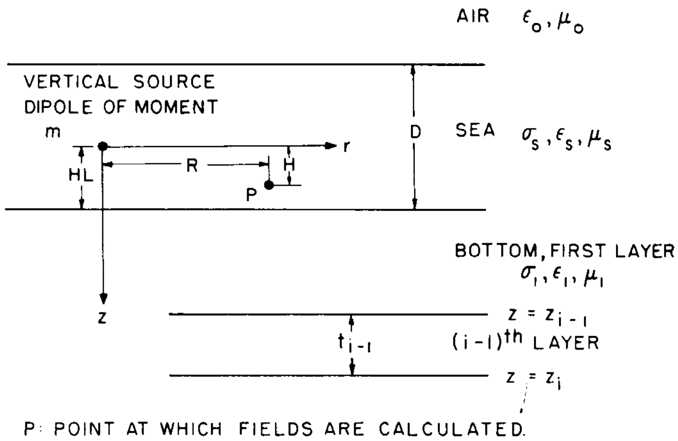


FIG. 1. Geometry for dipole in the sea.

several quantities that depend markedly on bottom properties. However, these solutions hold only for the "quasi-near" range, where measurement distance is much less than a free space wavelength but much greater than sea and seabed skin depths, and where the horizontal separation is much greater than the depth of source and receiver. Shakhsuvarov and Zvereva (1967) set out the expressions necessary for exact calculation of fields of dipoles set in a series of conductive layers, but some computational results in a later paper (1968) are for asymptotic behavior under conditions similar to those enforced by Bannister.

In this paper an attempt is made to analyze fields about a vertical magnetic dipole. Such a source may approximate the loop transmitter of a geophysical system comparable to those used at present for mineral exploration and sounding on land. As the integral expressions derived for the fields are evaluated numerically, no limits on the sea depth or measurement distance relative to sea or bottom skin depths are necessary. Some interesting behavior is observed when the fields are calculated for a wide range of parameters. Analysis of the results is aimed at understanding the field behavior and utilizing this behavior for measurement of sea bottom conductivities.

## COMPUTATION OF FIELDS

The air, sea, and bottom are represented mathematically by a series of horizontal layers, in each of which the conductivity $\sigma$, permittivity $\epsilon$, and permeability $\mu$ are constant (Figure 1). A vertical magnetic dipole is set in the sea; in this situation there are only three field components produced—horizontal electric $E_T$ (circular about the vertical axis), vertical magnetic $H_Z$, and horizontal magnetic $H_R$ (radial about the vertical axis).

Manipulation of Maxwell's equations, in cylindrical coordinates, leads to the following:

$$H_R = -\frac{i}{\omega\mu}\frac{\partial E_T}{\partial z},$$

$$H_Z = \frac{i}{\omega\mu r}\frac{\partial}{\partial r}(rE_T), \tag{1}$$

$$\frac{\partial}{\partial r}\left[\frac{1}{r}\frac{\partial}{\partial r}(rE_T)\right] + \frac{\partial^2 E_T}{\partial z^2} + (\omega^2\mu\epsilon - i\omega\mu\sigma)E_T = S,$$

where a time dependence of $e^{i\omega t}$ is assumed, mks units are used, and $S$ is a source term. For a dipole of moment $m$ represented spatially by a delta function,

$$S = \frac{-i\omega\mu m}{2\pi}\delta(z)\frac{\partial}{\partial r}\left(\frac{\delta(r)}{r}\right). \tag{2}$$

It is convenient to apply a Hankel transform to the differential equation for $E_T$,

$$E_T(\lambda, z) = \int_0^\infty E_T(r, z)J_1(\lambda r)rdr, \tag{3}$$

to obtain the general form of the solution in $(\lambda, z)$ space:

$$E_T(\lambda, z) = F(\lambda)e^{\pm zu}, \quad (4)$$

where

$$u = [\lambda^2 - (\omega^2\mu\epsilon - i\omega\mu\sigma)]^{1/2}.$$

$J_1(\lambda r)$ is the Bessel function of order one and $F(\lambda)$ is a function of the transform variable $\lambda$.

The nature of the source and the maintenance of continuity of horizontal $E$ and $H$ fields at interfaces determine the solutions in each layer. The fields at a point $P$ ($r=R$, $z=H$, Figure 1) in the sea, with inverse Hankel tranformation, are found to be

$$E_T = \frac{-i\omega\mu_s m}{2\pi}\int_0^\infty \frac{A(\lambda)}{u_s} J_1(\lambda R)\lambda^2 d\lambda, \text{ (a)}$$

$$H_Z = \frac{m}{2\pi}\int_0^\infty \frac{A(\lambda)}{u_s} J_0(\lambda R)\lambda^3 d\lambda, \text{ (b)} \quad (5)$$

$$H_R = \frac{m}{2\pi}\int_0^\infty \frac{A(\lambda)}{T_H} J_1(\lambda_R)\lambda^2 d\lambda, \text{ (c)}$$

where $u_s$ is $u$ for the sea,

$$A(\lambda) = e^{-u_s H} T_H \left[\frac{(T_s+1)+(T_s-1)e^{-2u_s(D-HL)}}{(T_s+1)(T_H+1)-(T_s-1)(T_H-1)e^{-2u_s(D-HL+H)}}\right],$$

$$T_s = Z_{(\text{air/sea})}/X_{(\text{sea})},$$

$$T_H = Z_{(z=H)}/X_{(\text{sea})}.$$

$Z$ = surface impedance, equal to total $E_T/H_R$ at a surface. Thus $X = -i\omega\mu/u$ = intrinsic impedance of a medium, equal to $E_T/H_R$ for downward traveling waves [in $(\lambda, z)$ space].

Impedances at interfaces are related to each other (see Figure 1 for layer notation):

$$Z_{i-1} = X_{i-1}\left[\frac{Z_i + X_{i-1}\tanh(t_{i-1}u_{i-1})}{Z_i\tanh(t_{i-1}u_{i-1}) + X_{i-1}}\right], \quad (6)$$

so any surface impedance can be calculated from intrinsic impedances. (Note $Z_i = X_i$ at the deepest interface, and $Z_i = -X_o$ at the sea-air interface.)

Field values have been computed by numerically integrating equations (5). With $H$ nonzero, the integrands attenuate with the factor $e^{-u_sH}$, so finite integrals well approximate the infinite ones. When $H$ is zero, however, it is necessary to consider the asymptotic forms of the integrands [$A(\lambda)\to\frac{1}{2}$ as $\lambda\to\infty$] so that these may be subtracted during numerical integration, then integrated analytically and added on.

Two simplifications have been made: permeability is everywhere that of free space, and displacement currents are negligible in the sea and sea bottom (this is true for the frequencies and conductivities considered).

All the results are presented in dimensionless form. Independent variables are (i) sea induction number, $\theta = (\omega\mu_o\sigma_s)^{1/2} R$, (ii) bottom/sea conductivity ratio(s), $k = \sigma(\text{bottom})/\sigma(\text{sea})$, and (iii) geometrical parameters, $D/R$, $HL/R$, etc. (see Figure 1). Dimensionless field quantities are functions of the above, and true fields may be obtained as follows: electric field $= (m\omega\mu_o/4\pi R^2)\times$ dimensionless "electric field"; and magnetic field $= (m/4\pi R^3)\times$ dimensionless "magnetic field." The dimensionless fields are thus the values relative to quasi-static fields in free space at $z=0$, $r=R$.

#### BEHAVIOR OF FIELDS

The range of sea induction numbers for which the fields appear most interesting and suitable for measurement of bottom conductivities is from about one to a few hundred. Since the number of wavelengths in $R = 0.112\ \theta$ and the number of skin depths in $R = 0.707\ \theta$, the range of one to a few hundred corresponds to distances from the source of 0.1 to 10 and more sea wavelengths or 0.7 to 70 and more sea skin depths. Bottoms with conductivities from 3 to $10^{-4}$ times that of seawater (about 4 mhos/m) have been considered, as these values should cover the range of common geological cases.

Figure 2 shows the in-phase electric field as a function of $\theta$ for several conductivities of sea bed (a half-space), with $D/R = 0.2$ and source and receiver on the bottom. Certain features are characteristic of all the field components: (1) peak field strength occurs between $\theta = 1$ and 10; (2) there is strong attenuation beyond $\theta = 10$, especially for conductive bottoms; and (3) sea-bed conductivity significantly affects response for $k$ greater than about $10^{-2}$.

The in-phase horizontal magnetic field, for the

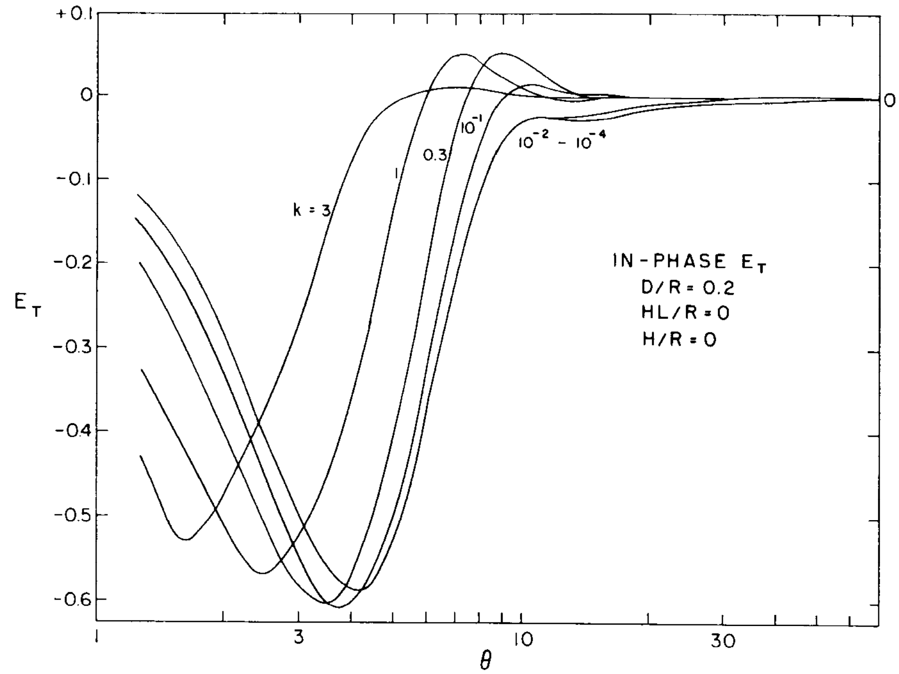


FIG. 2. In-phase electric field for various sea bottoms. The sea bottom is assumed to be a uniform half-space; the transmitter and receiver are on the bottom; sea depth/horizontal separation is 0.2.

same geometry, is plotted in Figure 3. Two other features stand out more clearly than for the electric component: (1) the responses for less conductive bottoms ($k=10^{-2}-10^{-4}$) are distinguishable at increasing induction numbers ($\theta>10$, say); and (2) there is a "kink" apparent in the curves for $k=10^{-2}-10^{-4}$, at about $\theta=10$–15.

Both horizontal electric and magnetic fields respond to poorly conducting bottoms for $\theta$ greater than about 10, but the vertical magnetic field does not (see following section and Figure 7). The "kinks" in the response curves shed some light on the propagation paths.

The amplitude of the horizontal magnetic field is shown in Figure 4 for several sea depths and $k$ of $10^{-4}$. It is seen that as sea depth increases, the position of the kink and main peak move toward smaller induction numbers and the amplitude of the kink decreases. This behavior suggests that, with a *poorly conducting seabed*, the total horizontal fields result from energy propagating in two main ways: through the bottom and through the air just above the sea surface.

Such a concept is borne out by the curves of Figure 5. The component—out-of-phase horizontal magnetic—for all the situations shown is entirely caused by vertical changes in conductivity, for it would be zero in a uniform whole space (receiver at the same height as dipole). When the response at the bottom of a very deep sea (curve $A$) is subtracted from that for a shallow sea ($D/R=0.2$, curve $B$), the result ($B-A$) is very similar to the response obtained at a depth 0.2 $R$ in a bottomless sea (curve $C$). That is, the effects of sea/air and sea/bottom interfaces are roughly additive, an indication that little energy is guided through the sea (e.g. by reflection). The minor coupling that is indicated probably consists of energy leakage between the bottom and the air.

For the case shown ($D/R=0.2$), the "air wave" contribution is insignificant beyond $\theta=20$, no doubt because of attenuation through the sea from source to surface and back to the bottom. The easily visible kinks in the response curves are in the region of the transition from where both "air" and "bottom" waves are important to where practically all energy appears to have travelled through the bottom.

The kink in the vertical magnetic field response (evident from the amplitude contours at $\theta=10$–20

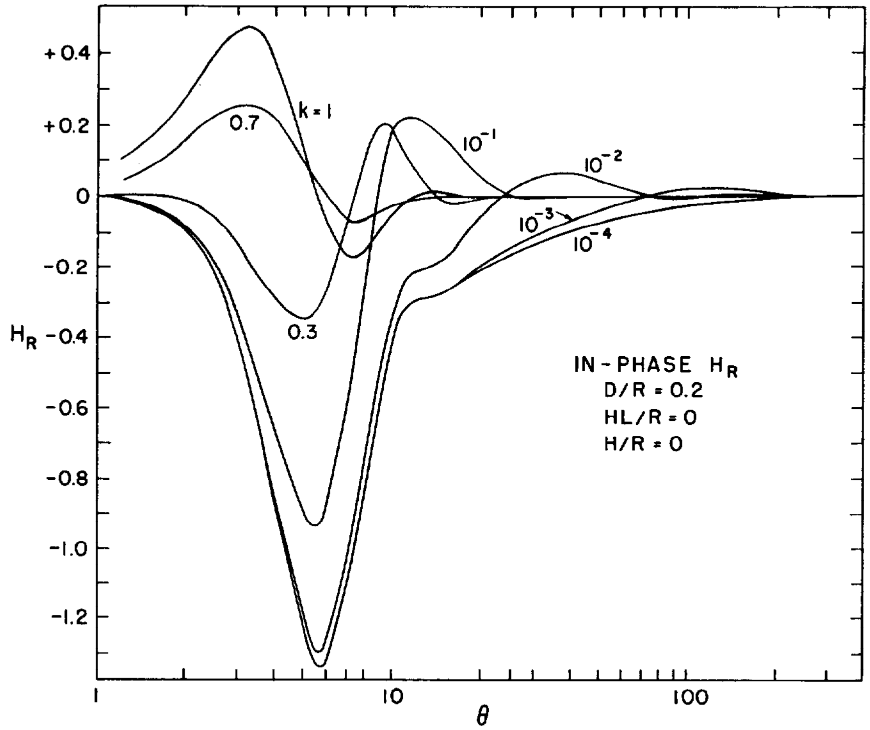


FIG. 3. In-phase horizontal magnetic field for various sea bottoms. The sea bottom is assumed to be a uniform half-space; the transmitter and receiver are on the bottom; sea depth/horizontal separation is 0.2.

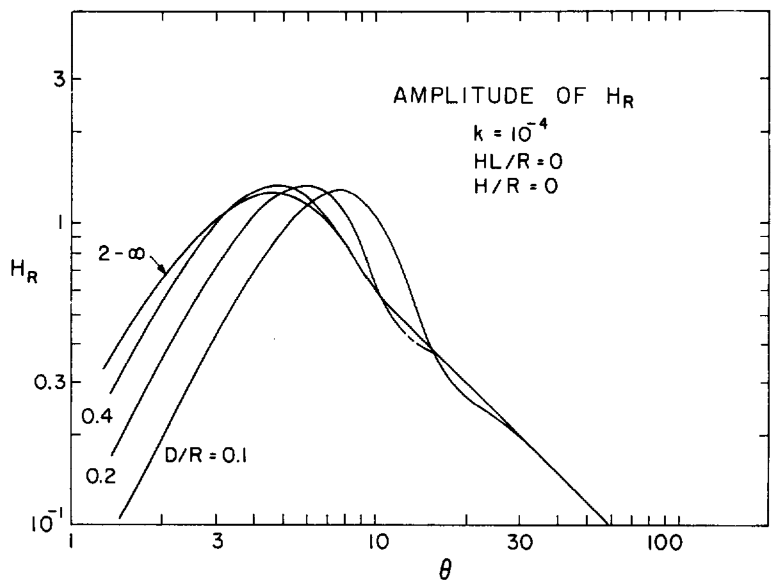


FIG. 4. Horizontal magnetic field amplitude response as a function of relative sea depth, $D/R$. The response is practically independent of $D/R$ when this is greater than 2. The sea bottom is assumed to be a uniform half-space with conductivity ratio $k=10^{-4}$; the tramsmitter and receiver are on the bottom.

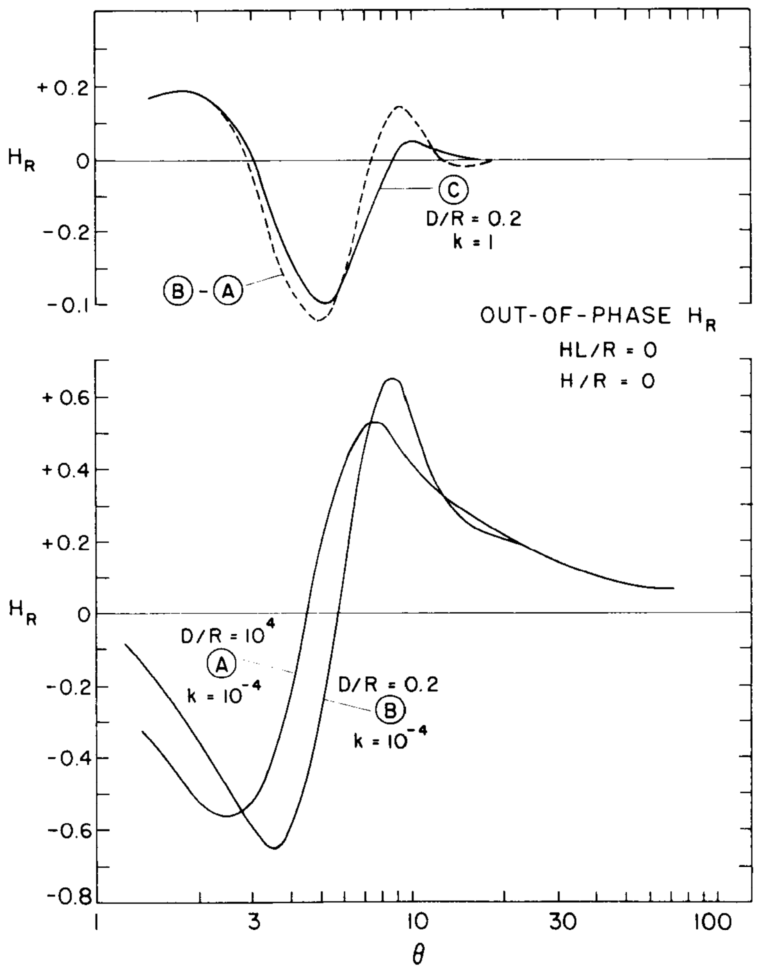


FIG. 5. Demonstration that total out-of-phase horizontal magnetic field response is approximately the simple sum of air and bottom path contributions. (B) represents the total effects of bottom and sea/air interfaces. (A) shows the contribution from the bottom only. The difference, (B)—(A), representing the air contribution, is compared with (C), which is the actual effect of the sea/air interface alone.

in Figure 7) again indicates interference between reflections or refractions from the two interfaces. However, it was not found possible to relate the interface effects as simply as those for the horizontal field. From the very small amplitudes (relative to those of the horizontal magnetic component) at large induction numbers even over poorly conducting bottoms, it is apparent that propagation through the bottom does not contribute much to the vertical field.

Further sea depth effects are shown in Figure 6, for the amplitude of the horizontal magnetic field. Bottoms less conductive than the sea tend to be a little better separated at the smaller values of $D/R$, but this effect is not important. (See also Figure 12 and discussion on measurement of bottom conductivity.)

Sea depth strongly affects field strength when $D/R$ is small. However, the variation (increase or decrease as depth increases) depends on induction number and bottom conductivity, as may be seen in Figures 4 and 6. For depths greater than some minimum which is a function of induction number (e.g. $D/R$ about 0.3 for $\theta = 20$), all fields are sensibly independent of sea depth. In practice it may often be desirable to operate with $D/R$ above

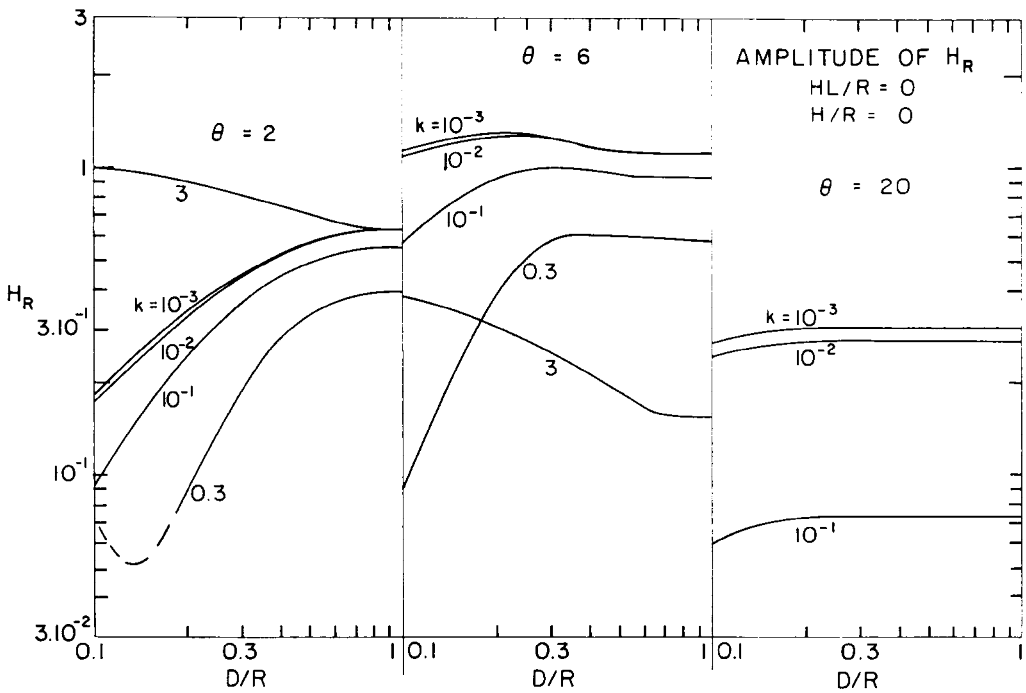


FIG. 6. Effects of sea depth on horizontal magnetic field amplitude for various sea bottoms. The sea bottom is assumed to be a uniform half-space; the transmitter and receiver are on the bottom.

this minimum so that variations in sea depth can be neglected.

## MEASUREMENT OF BOTTOM CONDUCTIVITY

### *Homogeneous sea bottoms*

To illustrate the scope for determining bottom conductivity, diagrams of responses over the range $\theta=1$ to 300 and $k=10^{-4}$ to 3 are given. The geometry is $D/R=0.2$ and both transmitter and receiver are on the sea floor.

The vertical magnetic field amplitude is contoured in Figure 7. This field is characteristically insensitive to bottoms with $k$ less than $10^{-1}$–$10^{-2}$ and attenuates rapidly with increasing induction number. It does look useful for measurement of conductivities represented by $k>10^{-1}$.

The horizontal magnetic field, as seen in Figure 8, shows more promise for less conductive bottoms. However, for $\theta$ less than 10, two conductivity ratios $k$ may give equal field amplitudes.

The horizontal field is usually 5–10 or more times the vertical component for $\theta$ greater than 20; and for large $\theta$, too, the value of the field is sensitive to changes in $k$ for small $k$ ($10^{-2}$–$10^{-4}$). These two desirable features result from propagation chiefly through the sea-bed.

Phase of the horizontal field shows a very simple variation with induction number ($\theta>20$) and conductivity ratio ($k\leq 10^{-1}$), as seen in Figure 9. This useful behavior approximates that for plane waves, where (phase angle) = (wave number) × (distance) + (constant). For the sea-bed, (wave number) × (distance) $=\theta(k/2)^{1/2}$ and actual (phase angle/$\theta$) slopes are roughly $(k/2)^{1/2}$.

As evident from Figure 2, the electric field is also sensitive to conductivity variations, to $k$ greater than $10^{-1}$–$10^{-2}$ where $\theta$ is less than 10, and to $k$ less than $10^{-2}$ for larger $\theta$. Very small amplitudes, however, make the electric field less attractive than the horizontal magnetic field.

Other quantities, such as field ratios, tilt of polarization ellipse, etc., appear no more useful than the simple field amplitudes or phases. Some show more complicated behavior as functions of induction number and conductivity and are more difficult to analyze or use.

Although the optimum theoretical arrangement is to have transmitter and receiver on the sea-

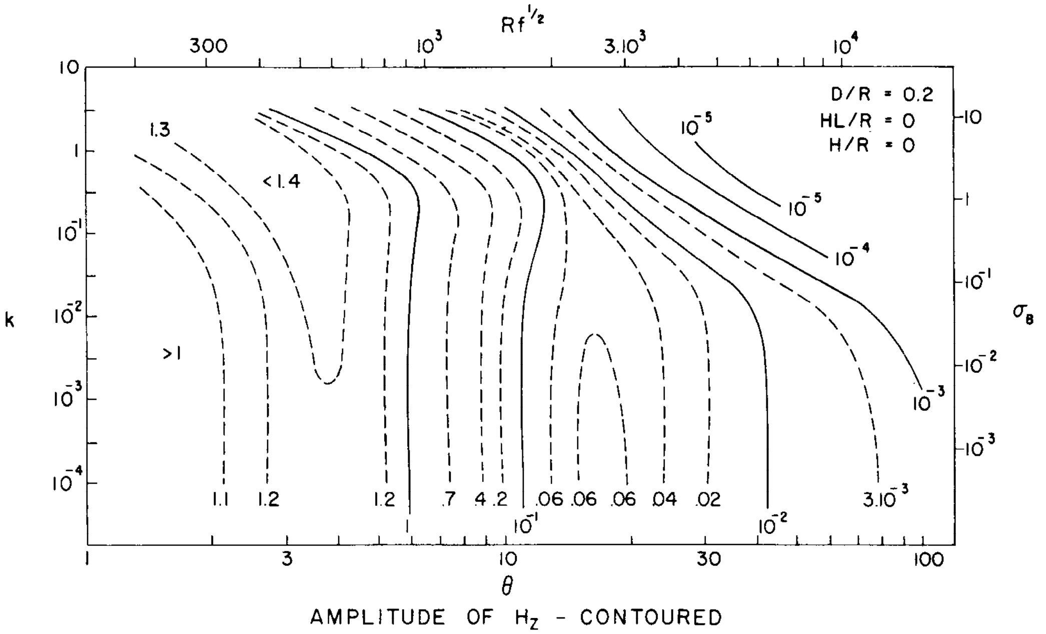


FIG. 7. Contour plot of vertical magnetic field amplitude versus sea induction number $\theta$ and bottom conductivity ratio $k$. Sea bottom is assumed to be a uniform half-space. Contours are drawn from interpolation of profiles calculated for several values of $k$. Scales $Rf^{1/2}$ ($f$=frequency) and $\sigma_B$ (bottom conductivity) correspond to those for $\theta$ and $k$ respectively when seawater conductivity is 4 mhos/m.

floor, there may be practical advantages in keeping them above the bottom—for example, so as to carry out continuous profiling. Effects of such a geometry, where (source height) $R$ is 0.02, are shown in Figure 10. This diagram should be compared with Figure 8. It is seen the general char-

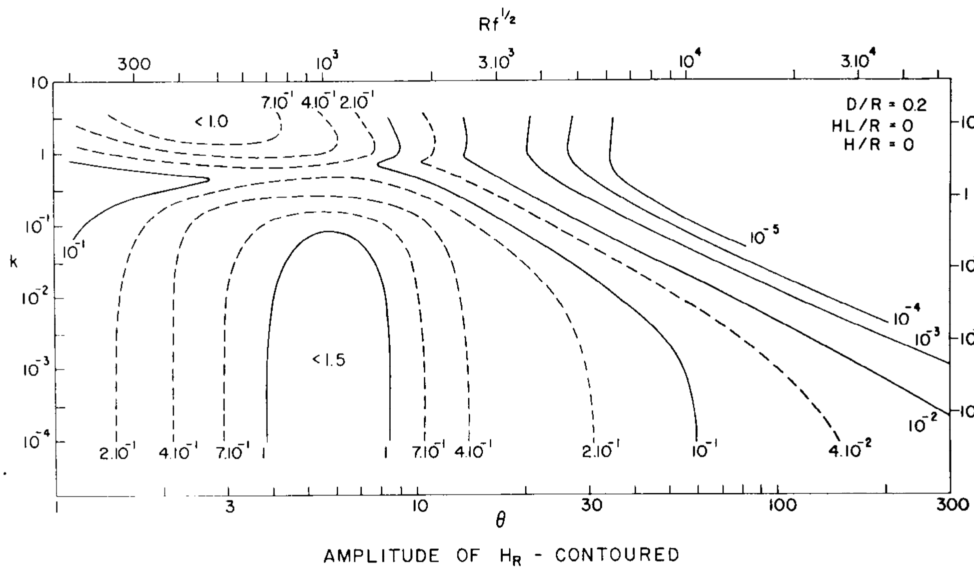


FIG. 8. Contour plot of horizontal magnetic field amplitude versus sea induction number $\theta$ and bottom conductivity ratio $k$. Sea bottom is assumed to be a uniform half-space.

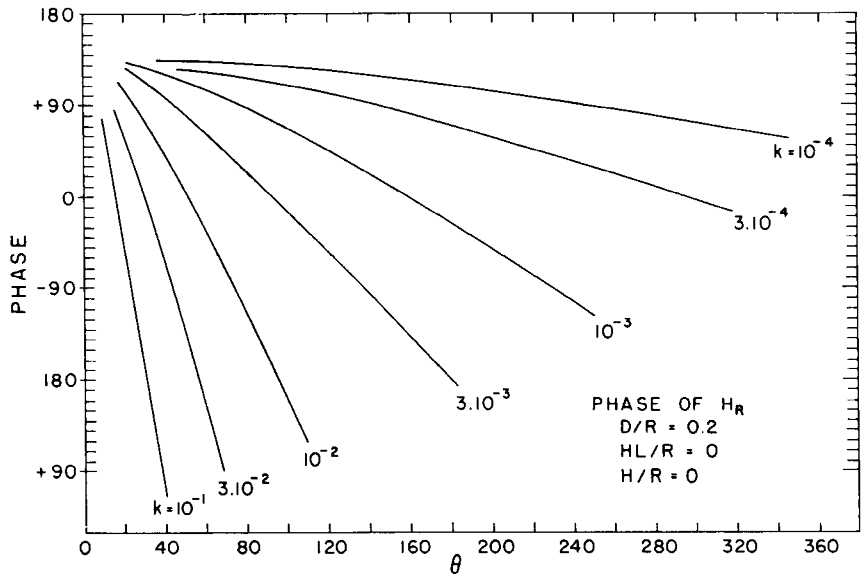


FIG. 9. Phase of horizontal magnetic field versus sea induction number $\theta$ and bottom conductivity ratio $k$. Sea bottom is assumed to be a uniform half-space.

acter of the responses is the same, the main result of elevation above the bottom being an attenuation, which increases with induction number. It is this attenuation, rather than impairment of sensitivity to small $k$'s as evidenced by slopes of contours, that is the disadvantage of not being on the bottom. But for $k$ greater than $10^{-1}$, changes are minor.

Phase angle variation of the horizontal magnetic field for $\theta > 20$ (Figure 11) retains the simple

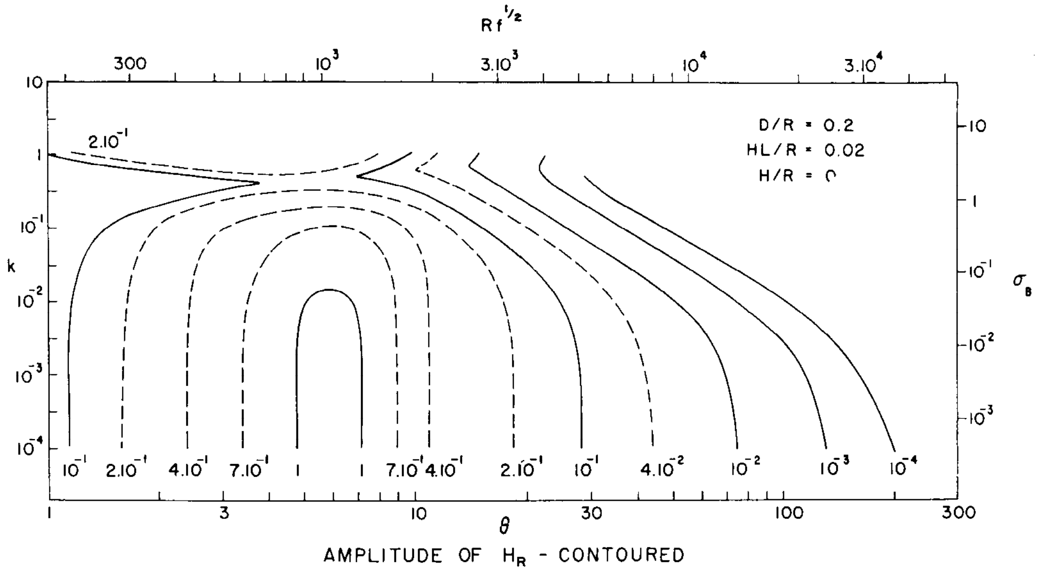


FIG. 10. Contour plot of horizontal magnetic field amplitude versus sea induction number $\theta$ and bottom conductivity ratio $k$ when source and receiver are above the sea bottom (a uniform half-space). Transmitter height/horizontal separation is 0.02.

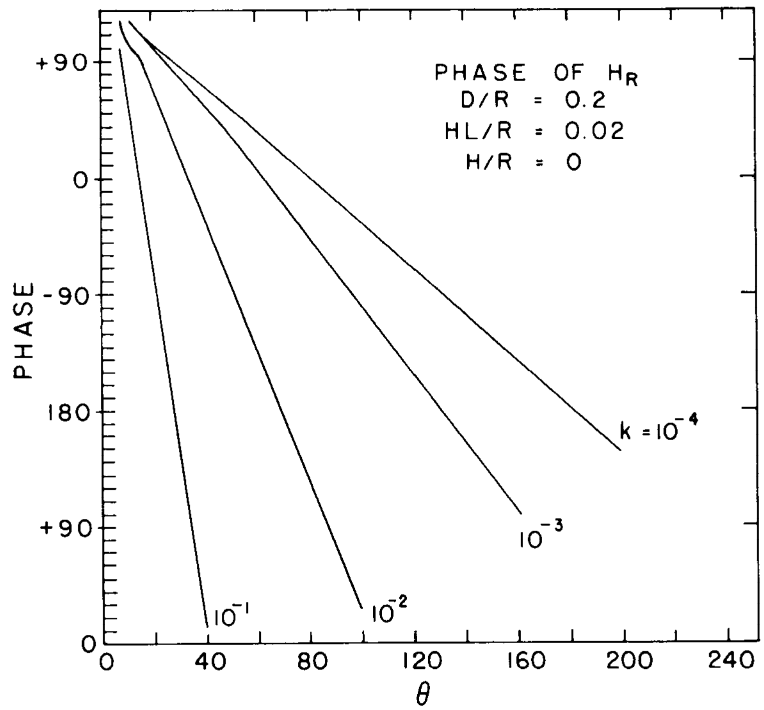


FIG. 11. Phase of horizontal magnetic field versus sea induction number $\theta$ and bottom conductivity ratio $k$ when source and receiver are above the sea bottom (a uniform half-space). Transmitter height/horizontal separation is 0.02.

form of that for zero height (Figure 9). The steeper slopes may be expected from the relation (for plane waves):

$$\begin{aligned}\text{(phase angle)} &= \text{(sea wavenumber)}\\ &\quad \times \text{(distance in sea)}\\ &\quad + \text{(bottom wavenumber)}\\ &\quad \times \text{(distance in bottom)}\\ &\quad + \text{(constant)}\\ &= \theta(C_1 + C_2 \cdot k^{1/2}) + C_3\\ &\quad (C\text{'s are constants}).\end{aligned}$$

The coefficient of $\theta$ is greater than for the case of zero height.

As mentioned earlier, sea depth has little effect on sensitivity to bottom conductivity. This is evident from a comparison of Figures 8 ($D/R=0.2$) and 12 ($D/R=2.0$) showing the horizontal magnetic field amplitude. Although there are differences, especially in the ranges $k>0.1$ and $\theta<10$, the general form of the contours is very similar in the two diagrams. Thus, the choice of induction numbers suitable for measurement of a given range of conductivities is not affected by $D/R$.

*Layered bottoms*

Two examples of layered bottoms show that layering is clearly distinguishable from a homogeneous half-space. To illustrate the differences, we found apparent-conductivity ratios, $k_A$, Figures 7–9. The apparent ratio is the value of $k$ that a homogeneous sea bottom would need to have in order to yield a response equal to that calculated for a layered model. Thus, a vertical field strength of $10^{-2}$ at induction number of 30 gives $k_A$ of $4\times10^{-2}$ from Figure 7.

A conductive layer ($k=0.3$) above half-spaces of lower conductivity gives the results shown in Figure 13. Although the variation of $k_A$ with induction number (or frequency) demonstrates inhomogeneity, interpretation promises to be more difficult than for a layered structure on land.

Another interesting model is that of a thin

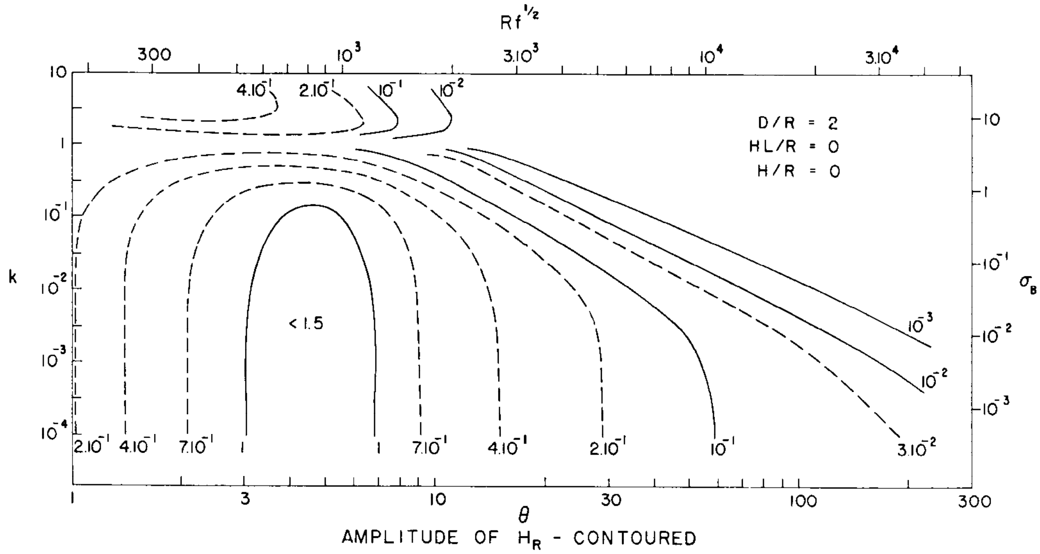


FIG. 12. Contour plot of horizontal magnetic field amplitude versus sea induction number $\theta$ and bottom conductivity ratio $k$ in a deep sea. Sea depth/horizontal separation is 2; transmitter and receiver are on the sea bottom, which is assumed to be a uniform half-space.

highly conducting layer at some depth in less conductive ground (Figure 14). This layer raises the apparent-conductivity well above that for the bulk bottom material, for "small" induction numbers (<20 for this model). As induction number is increased, $k_A$ decreases sharply.

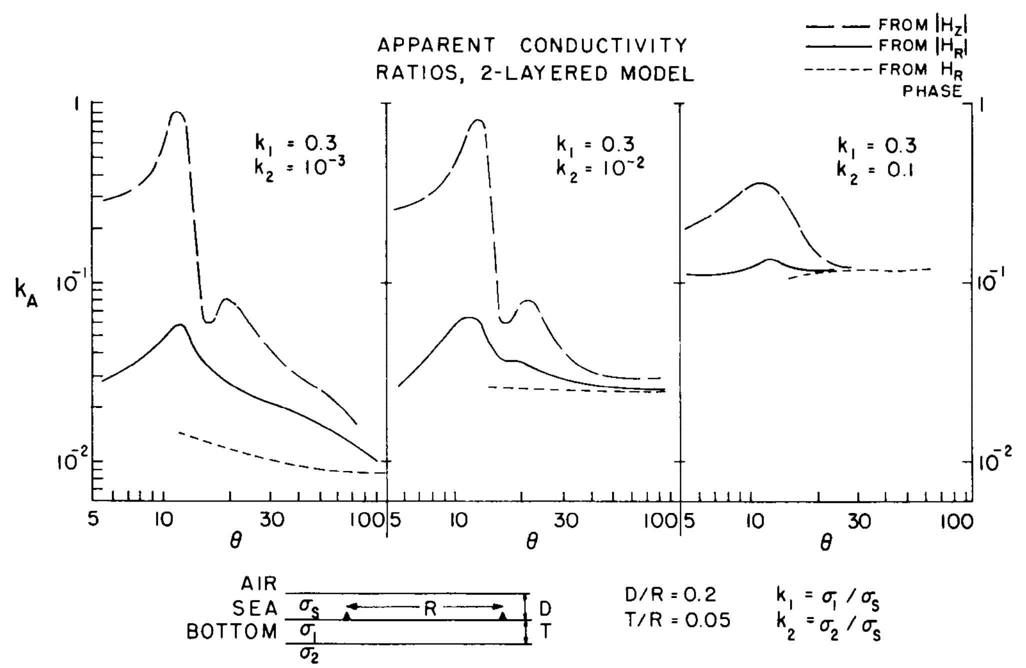


FIG. 13. Apparent conductivity ratios for a two-layered sea floor. Model is a thin conductive layer overlying a less conductive half-space. Transmitter and receiver are on the bottom.

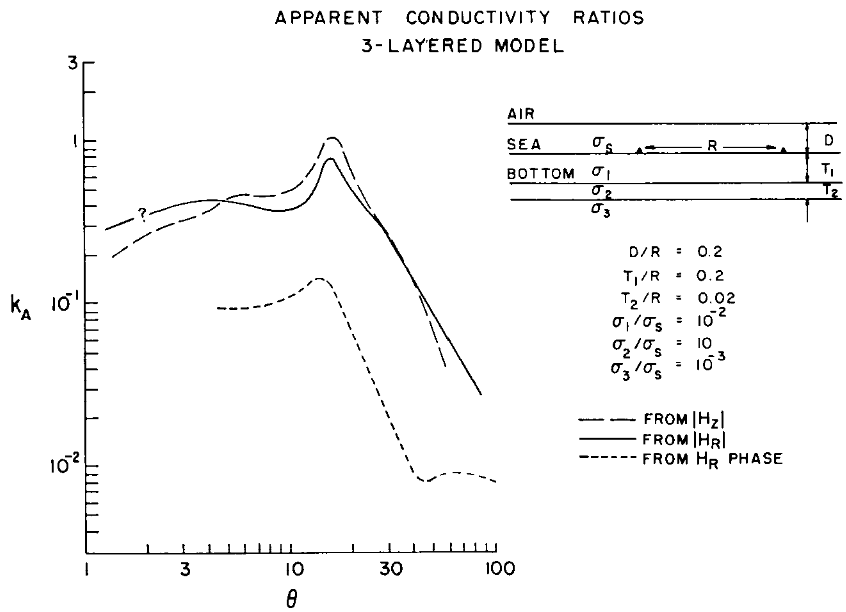


FIG. 14. Apparent conductivity ratios for a three-layered sea floor. Model is a thin conductive layer buried in poorly conducting material. The transmitter and receiver are on the bottom.

A possibly useful feature is that different quantities ($H_Z$ and $H_R$ amplitudes, $H_R$ phase) give differing apparent-conductivity ratios.

## DISCUSSION

The range of this analysis and application to seabed conductivity measurement may be summarized by considering three regions in terms of wavelength or induction numbers. It is assumed that the horizontal separation $R$ is much less than a free space wavelength.

(i) $R$ is greater than both sea and bottom wavelengths. [This range of $R$ corresponds to the upper right part of Figures 7, 8, 10, above ($\theta=10$, $k=1$) to ($\theta=300$, $k=10^{-3}$) and right of $\theta=10$.]

Fields are weak and vary in a relatively simple manner with bottom conductivity and $\theta$. For small $k$, only the horizontal fields are significant, because of radiation through the bottom; while propagation through the air may be important for more conductive bottoms and when $D/R \ll 1$. The higher part of this range corresponds to the "quasi-near" range treated by Bannister (1968b) by means of approximations.

(ii) $R$ is greater than sea wavelength, less than bottom wavelength. This range of $R$ corresponds to the lower right in Figure 8, below ($\theta=10$, $k=1$) to ($\theta=300$, $k=10^{-3}$) and right of $\theta=10$.

The fields represent the combination of rapid attenuation and phase change of sea and sea-air paths and near-field type response of the bottom. Amplitudes are greater than for (i); that part of this division nearer (i) looks most useful for bottom conductivity measurements when $k$ is less than $10^{-1}$.

(iii) $R$ is less than both sea and bottom wavelengths. (This range of $R$ corresponds to the left part of Figure 8, $\theta$ less than 10.)

The fields of this range have the largest amplitude of all. They are useful for measurement of the conductivity of seafloors with $k$ greater than about 0.03. Less conductive bottoms, however, have little inductive effect and cannot be differentiated.

Another division, $R$ less than sea wavelength but greater than bottom wavelength, only includes bottoms more conductive than the sea (top center of Figure 8, $\theta$ less than 10). As a seabed (half-space) of such conductivity is unlikely, values for $k$ above 3 were not calculated.

It is concluded that to have the capability of measuring bottom conductivities in the entire range $k=3$ to $10^{-4}$, a spread of frequencies suitable for sea induction numbers of 2 to 200 is required. The amplitude and phase of the horizontal magnetic field promise to be the most useful quantities. For measurements on the sea floor, total signals no less than 1/10 the static dipole vertical field strength should enable determination of conductivity ratios down to $10^{-3}$. The electric field may be strong enough to utilize at short separations and high frequencies; and for $k>10^{-1}$, the vertical magnetic field is useful.

In a practical marine electromagnetic (MEM) system, it would be simpler to use several frequencies at a fixed separation than to vary separation for sounding applications. Measurements at different frequencies may be plotted on a diagram such as Figure 8. For a homogeneous bottom, interpretation is a matter of fitting a straight line ($k$=constant) to the plotted points; marked deviation from a straight line would indicate inhomogeneity. A catalog of response curves, in profile form or contour form, would be a prerequisite to development of an interpretation method for two-layered sea bottoms.

The results of this analysis are sufficiently encouraging for some applications of a MEM system to be envisaged.

Electrical conductivity measurement of unconsolidated seafloor sediments can provide information on porosity and the type of sediment. Kermabon et al (1969) successfully used a resistivity probe for this purpose. An electromagnetic system may have the advantages of greater speed of measurement and of sampling a larger volume of sediment but would be unsuitable for determining details of layering. Since penetration depths desired are small (a few tens of meters at most), a coil separation of 30 m may be suitable. In many cases, sea depths would be greater than 30 m; and thus the sea-surface effects, negligible. Unconsolidated sediments, with porosities greater than 50 percent and saturated with seawater, have $k$ values in the range 0.25–1. Both vertical and horizontal magnetic fields are very sensitive to seabottoms of this type (as seen from Figures 7 and 12) for the range of sea induction numbers from 3 to 10. For $R$ of 30 m, this range corresponds to frequencies from 320 to 3500 hz. Lower frequencies may also be used, particularly with the vertical field.

Investigation of sediments in coastal areas—estuaries, bays—and lakes introduces the problem of small water depths. For instance, for the Great Salt Lake in Utah, a depth of 3 m and a separation of 30 m gives $D/R=0.1$. As $k$ for the bottom may again be taken to be 0.25–1, to maintain field strength, induction numbers should be less than 10 (a frequency of 730 hz for conductivity of 24 mhos/m). In this operating range, the water depth has a very strong effect on the fields, as seen for example in Figure 6 with $\theta=6$, $k=0.3$, $D/R=0.1$. Clearly then, (a) water depth must be known accurately; and (b) waves are likely to cause difficulty in making measurements.

Of greater application to geological studies, either scientific or applied, is the possibility of undersea electromagnetic sounding. Rocks of the continental shelves—indurated sediments, igneous and metamorphic rocks—are much less conductive than seawater, with $k$'s less than 0.1. Hence, use of the horizontal magnetic field at induction numbers greater than 10 is suggested. For a horizontal separation of 200 m, frequencies are 79 hz for $\theta=10$ and 7900 hz for $\theta=100$. Although with a 200 m separation, $D/R$ may be less than one (e.g. 0.2), the sea/air surface has little influence at the high induction numbers required. The ability to penetrate a thin conductive layer, such as unconsolidated sediments, and respond to less conductive material beneath is evident from Figure 13.

On the basis of general response to seabottom conductivity variations, use of a MEM system in searching for ore deposits also looks promising. In order to obtain strong total fields, to be insensitive to conductivity variations when $k<1$, but to detect good conductors, lower sea induction numbers than are best for conductivity mapping or sounding may be chosen. Though finite bodies cannot be treated here, a suggestion of the effects of a buried good conductor is given by Figure 14.

These results show there may be a wide range of application for marine electromagnetic methods.


## ACKNOWLEDGMENTS

We would like to thank Professor S. H. Ward and Dr. J. R. Parry for helpful comments and discussion relating to this study.

The University of California Computer Center, Berkeley, made available computing time on a CDC 6400 necessary for calculation of the results presented here.


## REFERENCES


Bannister, P. R., 1967, The quasi-near fields of dipole antennas: IEEE Trans. Ant. Prop., v. AP-15, p. 618–626.

——— 1968a, Electromagnetic fields within a stratified earth produced by a long horizontal line source: Radio Science, v. 3, p. 387–390.

——— 1968b, Determination of the electrical conductivity of the sea bed in shallow waters: Geophysics, v. 33, p. 995–1003.

Baños, A., 1966, Dipole radiation in the presence of a conducting half-space: Oxford, Pergamon Press.

Brock-Nannestad, L., 1965, Determination of the electric conductivity of the sea bed in shallow waters with varying conductivity profile: Electronics Letters, v. 1, p. 274–276.

Burrows, C. R., 1963, Radio communication within the earth's crust: IEEE Trans. Ant. Prop., v. AP-11, p. 311–317.

Kermabon, A., Gehin, C., Blavier, P., 1969, A deep-sea electrical resistivity probe for measuring porosity and density of unconsolidated sediments: Geophysics, v. 34, p. 554–571.

Moore, R. K., 1967, Radio communication in the sea: IEEE Spectrum, v. 4, p. 42–51.

Mott, H., and Biggs, A. W., 1963, Very low frequency propagation below the bottom of the sea: IEEE Trans. Ant. Prop., v. AP-11, p. 323–329.

Shakhsuvarov, D. N., and Zvereva, E. V., 1967, An algorithm for the calculation of electromagnetic fields generated by dipole sources buried in conducting stratified media: Bull. (Izv.) Acad. Sci. U.S.S.R., Physics of the Solid Earth, p. 603–605, (English ed.).

——— 1968, Some results of calculations of the asymptotic behavior of the electromagnetic fields of immersed sources: Bull. (Izv.) Acad. Sci. U.S.S.R., Physics of the Solid Earth, p. 434–439, (English ed.).